第 34 卷第 6 期 无 机 化 学 学 报 Vol.34 No.6
2018 年 6 月 CHINESE JOURNAL OF INORGANIC CHEMISTRY 1121-1126

基于 3-吡唑-5 吡啶-1,2,4-三唑和均苯四甲酸构筑的两个同构配位聚合物的晶体结构和磁性

王玉芳*,[1] 太军慧[2] 颜小伟[1] 赵梦云[1] 王利亚*,[2]
([1]洛阳师范学院化学化工学院,功能导向多孔材料重点实验室,洛阳 471934)
([2]南阳师范学院化学与制药工程学院,南阳 473000)

摘要:以 3-吡唑-5 吡啶-1,2,4-三唑(H_2L)和均苯四甲酸(H_4btec)为配体合成了 2 个新的同构配位聚合物$[M(btec)_{0.5}(H_2L)]_n$ (M=Co(Ⅱ) (**1**),Cu(Ⅱ) (**2**)),通过 X 射线单晶衍射、元素分析、红外光谱等进行了结构表征。晶体结构分析表明配合物 **1** 和 **2** 是同构的,都属于正交晶系,空间群为 *Pbca*。2 个配位聚合物都是二维结构,通过 N…H…O 氢键形成三维超分子框架结构。此外对上述配合物进行了磁性研究,结果表明配合物 **1** 内通过羧基桥连的金属钴离子之间是弱的铁磁相互作用;配合物 **2** 中存在典型的顺磁行为。

关键词:同构;晶体结构;磁性
中图分类号:O614.121;O614.81+2 **文献标识码**:A **文章编号**:1001-4861(2018)06-1121-06
DOI:10.11862/CJIC.2018.135

Crystal Structures and Magnetic Properties of Two Isomorphic Frameworks Based on 3-(1*H*-pyrazol-4-yl)-5-(pyridin-2-yl)-1,2,4-triazole and 1,2,4,5-Benzenetetracarboxylic Acid

WANG Yu-Fang*,[1] TAI Jun-Hui[2] YAN Xiao-Wei[1] ZHAO Meng-Yun[1] WANG Li-Ya*,[2]
([1]*College of Chemistry and Chemical Engineering, Henan Key Laboratory of Function-Oriented Porous Materials, Luoyang Normal University, Luoyang, Henan* 471934, *China*)
([2]*College of Chemistry and Pharmaceutical Engineering, Nanyang Normal University, Nanyang, Henan* 473000, *China*)

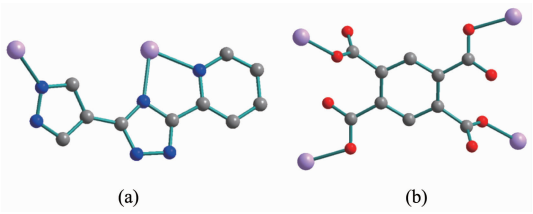
Abstract: Two new isomorphic coordination polymers, $[M(btec)_{0.5}(H_2L)]_n$ (M=Co(Ⅱ) (**1**), Cu(Ⅱ) (**2**); H_4btec=1,2,4,5-benzenetetracarboxylic acid; H_2L=3-(1*H*-pyrazol-4-yl)-5-(pyridin-2-yl)-1,2,4-triazole), have been synthesized under hydrothermal conditions. Compounds **1** and **2** were structurally characterized by elemental analysis, single crystal X-ray diffraction analysis, infrared spectroscopy and powder X-ray diffraction analysis. Single crystal X-ray diffraction measurement reveals that compounds **1** and **2** are isostructural structure and all crystallize in the orthorhombic system, space group *Pbca*. Compounds **1** and **2** have same 2D structure, which are connected by N…H…O hydrogen bonds to generate 3D frameworks. In addition, magnetic studies indicate that **1** show weak ferromagnetic exchange through carboxylate bridges between metal ions, and there is typical paramagnetic behavior in **2**. CCDC: 1559405, **1**; 1559419, **2**.

Keywords: isomorphic; crystal structure; magnetic property

收稿日期:2017-10-19。收修改稿日期:2018-03-27。
国家自然科学基金(No.21671114)资助项目。
*通信联系人。E-mail:wangyf78@163.com

0 Introduction

The keen interest in the design and fabrication of coordination polymers (CPs) has flourished as an emerging area of research because of their impressive structural topologies and promising application in guest molecule inclusion, gas and vapor storage, chemical sensing, magnetism, heterogeneous catalysis, *etc*[1-5]. Over the past decades, numerous CPs have been successfully constructed, and crystal engineering has reached a relatively mature level that some CPs with specific topologies can be designed by the judicious selection of metal ions and organic ligands[6-7]. In this regard, a very promising approach is the use of mixed ligands such as N-donor heterocyclic ligands together with polycarboxylate organic co-linkers in the same system[8-11]. N-donor heterocyclic ligands, particularly pyrazole-based flexible or rigid linkers, are acclaimed for their high thermal stability and interesting structural topologies[12-14]. Aromatic polycarboxylates are used extensively as organic co-linkers since they often produce inherently rigid structures which have potential application in gas adsorption and storages[15]. Keeping this in mind, in this contribution, we report the syntheses and characterization of two new 2D isomorphic coordination polymers with 3-(1*H*-pyrazol-4-yl)-5-(pyridin-2-yl)-1,2,4-triazole and 1,2,4,5-benzenetetracarboxylic acid (Scheme 1). The compounds are formulated as $[Co(btec)_{0.5}(H_2L)]_n$ (**1**), $[Cu(btec)_{0.5}(H_2L)]_n$ (**2**).



Scheme 1 Coordination modes of H_2L and $btec^{4-}$

1 Experimental

1.1 General

All reagents used in the syntheses were of analytical grade. Elemental analyses for carbon, hydrogen and nitrogen were performed on a Vario EL Ⅲ elemental analyzer. The infrared spectra (4 000~600 cm^{-1}) were recorded by using KBr pellet on an Avatar™ 360 E. S. P. IR spectrometer. The powder X-ray diffraction patterns (PXRDs) were recorded with a Bruker AXS D8 Advance diffractometer using monochromated Cu $K\alpha$ radiation (λ=0.154 18 nm, 2θ=5°~50°), in which the X-ray tube was operated at 40 kV and 40 mA. Magnetic measurements were carried out with a Quantum Design MPMS XL-7 SQUID-VSM magnetometer. Pascal′s constants were used to determine the diamagnetic corrections.

1.2 Preparation of compounds 1 and 2

A mixture of $Co(NO_3)_2\cdot 4H_2O$ (0.30 mmol, 87.3 mg), H_2L (0.1 mmol, 21.2 mg), and H_4btec (0.2 mmol, 50.8 mg) was dissolved in 8 mL mixed solvent of CH_3CN/H_2O (1:4, *V*/*V*), then sealed in a 25 mL Teflon-lined stainless steel vessel and heated at 160 ℃ for 72 h. After cooling to room temperature, the dark red block crystals were obtained and then washed with alcohol for several times and filtered to give pure crystals of **1**. Anal. Calcd. for $C_{15}H_9CoN_6O_4$(%): C 45.47, H 2.29, N 21.21. Found(%): C 45.51, H 2.25, N 21.18. IR (KBr, cm^{-1}): 2 973, 2 901, 2 352, 1 745, 1 694w, 1 551, 1 458, 1 361, 1 053, 884 808, 732, 673. Compound **2** was obtained by hydrothermal procedure as that for the preparation of compound **1** only using $Cu(OAc)_2\cdot H_2O$ (0.1 mmol, 19.9 mg), distilled water and 125 ℃ instead of $Co(NO_3)_2\cdot 4H_2O$, mixed solvent of CH_3CN/H_2O and 150 ℃. Green block crystals of **2** were collected. Anal. Calcd. for $C_{15}H_9CuN_6O_4$(%): C 44.95, H 2.26, N 20.96. Found (%): C 44.89, H 2.23, N 20.91. IR (KBr, cm^{-1}): 2 985, 2 905, 2 366, 1 746, 1 709, 1 556, 1 513, 1 466, 1 350, 1 046, 883, 805, 733, 679.

1.3 X-ray crystallography

Diffraction intensity data of the single crystals of **1** and **2** were collected on a Rigaku oxford diffraction equipped with a graphite monochromated Mo $K\alpha$ radiation (λ=0.071 073 nm) by using the X-scan technique at 293(2) K. The structures were solved by direct methods and refined on F^2 by full matrix least squares using SHELXTL[16]. All non-hydrogen atoms were refined anisotropically. The hydrogen atoms were located by geometrically calculations, and their

thermal parameters were fixed during the structure refinement. Crystallographic data and details of refinement for compounds **1** and **2** are reported in Table 1. Selected bond distances and angles are given in Table 2.

CCDC: 1559405, **1**; 1559419, **2**.

2 Results and discussion

2.1 Crystal structure description

Single crystal X-ray analysis reveals that compounds **1** and **2** are isomorphic, and hence only the structure of **1** is given in the ensuing discussion.

Table 1 Crystal data and structure refinement for compounds 1 and 2

Compound	1	2
Empirical formula	$C_{15}H_9CoN_6O_4$	$C_{15}H_9CuN_6O_4$
Formula weight	396.21	400.82
Crystal system	Orthorhombic	Orthorhombic
Space group	*Pbca*	*Pbca*
a / nm	1.562 59(7)	1.547 75(6)
b / nm	1.162 10(5)	1.139 13(4)
c / nm	1.724 75(7)	1.779 80(8)
Volume / nm^3	3.132 0(2)	3.137 9(2)
Z	8	8
D_c / (g·cm^{-3})	1.681	1.697
Absorption coefficient / mm^{-1}	1.133	1.429
F(000)	1 600.0	1 616.0
2θ range for data collection / (°)	6.714~50.984	6.764~50.992
Index range	$-18 \leqslant h \leqslant 8, -15 \leqslant k \leqslant 13, -20 \leqslant l \leqslant 11$	$-18 \leqslant h \leqslant 13, -13 \leqslant k \leqslant 13, -16 \leqslant l \leqslant 21$
Reflections collected	9 140	9 590
Independent reflections	2 892 (R_{int}=0.026 7)	2 857 (R_{int}=0.028 3)
Data, restraint, parameter	2 892, 0, 243	2 857, 0, 235
Goodness-of-fit on F^2	1.038	1.084
Final R indexes [$I \geqslant 2\sigma(I)$]	R_1=0.033 6, wR_2=0.074 8	R_1=0.039 9, wR_2=0.093 2
Final R indexes (all data)	R_1=0.043 4, wR_2=0.078 4	R_1=0.046 7, wR_2=0.096 1
Largest diff. peak and hole / (e·nm^{-3})	590 and −370	470 and −460

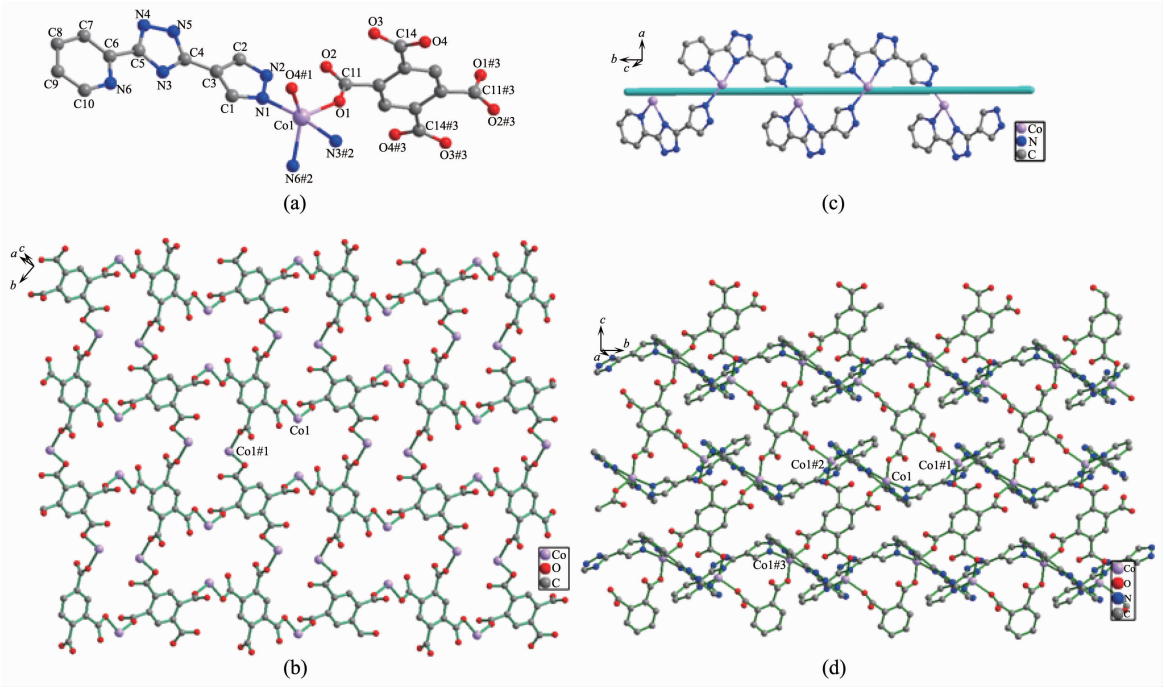
Table 2 Seclected bond lengths (nm) and bond angles (°) for compounds 1 and 2

1					
Co(1)-O(1)	0.204 06(16)	Co(1)-N(1)	0.212 6(2)	O(4)-Co(1)#1	0.203 02(17)
Co(1)-O(4)#1	0.203 03(17)	N(6)-Co(1)#1	0.212 1(2)		
O(4)#2-Co(1)-N(6)#1	133.91(7)	O(4)#2-Co(1)-O(1)	112.77(7)	O(4)#2-Co(1)-N(1)	91.77(8)
N(6)#1-Co(1)-N(1)	96.99(8)	N(1)-Co(1)-N(3)#1	171.20(7)	O(4)#2-Co(1)-N(3)#1	87.27(8)
O(1)-Co(1)-N(6)#1	109.69(7)	N(6)#1-Co(1)-N(3)#1	77.55(7)		
2					
Cu(1)-O(1)	0.200 7(2)	Cu(1)-N(1)	0.211 8(3)	Cu(1)-N(5)#2	0.199 4(3)
Cu(1)-O(3)#1	0.218 1(2)	Cu(1)-N(2)	0.199 1(3)		
N(5)#2-Cu(1)-O(3)#1	98.07(10)	O(1)-Cu(1)-N(1)	135.76(10)	N(5)#2-Cu(1)-N(1)	94.16(11)
N(2)-Cu(1)-N(5)#2	171.79(11)	N(1)-Cu(1)-O(3)#1	108.09(10)	N(2)-Cu(1)-N(1)	79.89(10)
N(5)#2-Cu(1)-O(1)	89.78(11)	N(2)-Cu(1)-O(1)	90.58(10)		

Symmetry codes: #1: 1−x, −1/2+y, 3/2−z; #2: 1−x, 1/2+y, 3/2−z for **1**; #1: x, 3/2−y, −1/2+z; #2: 1−x, −1/2+y, 1/2−z for **2**.

The asymmetry unit contains one Co(Ⅱ) ion, half $btec^{4-}$ ligand, and one H_2L ligand (Fig.1a). Each Co(Ⅱ) center is penta-coordinated by three N atoms from two different H_2L ligands (Co(1)-N(1) 0.212 6(2) nm, Co(1)-N(3)#2 0.216 50(19) nm, and Co(1)-N(6)#2 0.212 1(2) nm) and two O atoms from two different $btec^{4-}$ ligands (Co(1)-O(1) 0.204 06(16) nm, Co(1)-O(4)#1 0.203 03(17) nm) showing a distorted trigonal bipyramid coordination geometry. The O-Co-N bond angles vary from 87.28(7)° to 133.90(7)°. The O-Co-O bond angle is 112.77(7)° matching those of previously reported cobalt (Ⅱ) compounds[17].

It is noteworthy that the H_4btec is completely deprotonated in the formation of the compound **1**. The four carboxyl groups of $btec^{4-}$ ligand in compound **1** exhibit the same coordination modes (μ_1-η^1:η^0, μ_1-η^1:η^0, μ_1-η^1:η^0, μ_1-η^1:η^0) (Scheme 1b) and link neighboring four Co(Ⅱ) ions forming two-dimensional $[Co_4(btec)]^{4+}$ structure with the Co⋯Co separations of 0.637 5 and 0.920 0 nm, respectively (Fig.1b). On the other hand, H_2L ligands adopt the μ_3-bridging +chelating modes (Scheme 1a) to bind two Co(Ⅱ) ions forming 1D helix chain with the Co⋯Co separations of 0.637 5 nm (Fig.1c). The H_2L ligands link the two-dimensional $[Co_4(btec)]^{4+}$ plane through Co-N coordination interactions to give a two-dimensional network as illustrated in Fig.1d. In the crystal packing, there are H-bonding interactions between triazole nitrogen atom and carboxyl groups of $btec^{4-}$ ligand (N(2)–H(2)⋯O(2): $d_{H\cdots O}$=0.172(3) nm, $d_{N\cdots O}$=0.262 5(3) nm, ∠N–H⋯O=173(3)°; N(5)–H(5)⋯O(3)#1: $d_{H\cdots O}$=0.199 nm, $d_{N\cdots O}$=0.281 8(3) nm, ∠N–H⋯O=159.9°, Symmetry codes: #1: 3/2–x, 1/2+y, z). Analysis of the crystal packing also reveals the presence of face to face $\pi\cdots\pi$ stacking contacts between the neighbouring 2D layers. The triazole ring (C4-N3-C5-N4-N5) and pyridyl ring (C6-C7-C8-C9-C10-N6) of the neighbouring layers are almost parallel to each other with the dihedral angle of 1.028°. The perpendicular distance between the involved pyridyl and coordinated triazole ring is 0.338 6 nm. The centroid-to-centroid distance between the involved pyridyl and coordinated triazole ring is 0.355 2 nm. As a result, these coordination layers are further extended along the c-axis via such secondary interactions to form a 3D supramolecular lattice.



Symmetry codes: #1: 1–x, –1/2+y, 3/2–z; #2: 1–x, 1/2+y, 3/2–z; #3: 1–x, –y, 1–z

Fig.1 (a) Coordination geometry of the Co(Ⅱ) ion in **1**; (b) 2D layer $[Co_4(btec)]^{4+}$ in **1**; (c) 1D chain $[Co(H_2L)]^{2+}$ in **1**; (d) 2D network of **1**

2.2 PXRD study

Phase purities of the materials of **1** and **2** were confirmed by powder X-ray diffraction (PXRD) patterns (Fig.2). The experimental and simulated PXRD patterns agree well with each other, confirming the good phase purity. The slight difference in intensity may arise from the preferred orientation of crystalline powder samples.

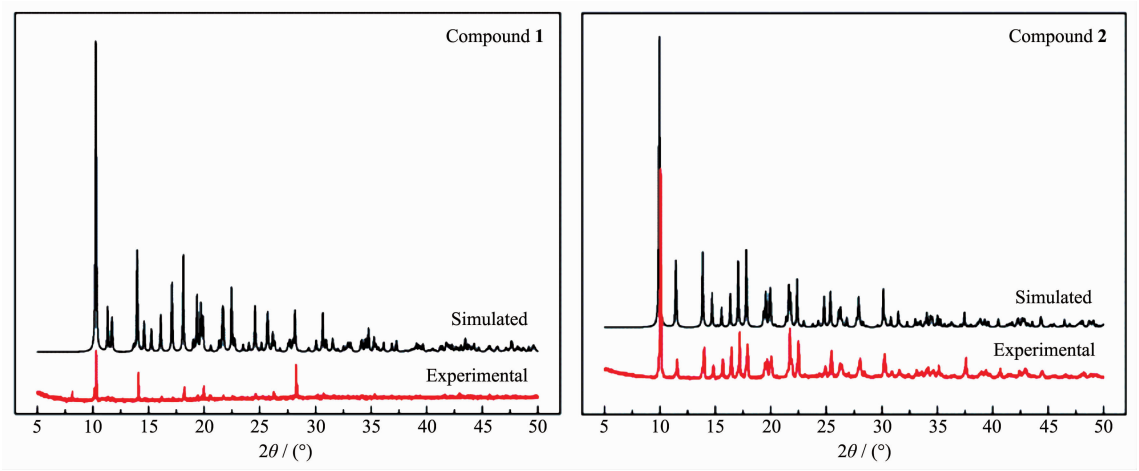


Fig.2　PXRD patterns of **1** and **2**

2.3 Magnetic properties of the compounds

According to the structural data, compound **1** contains Co(Ⅱ) chain interlinked by the H_2L and $btec^{4-}$ ligands. Considering the interchain Co⋯Co distance (0.637 5 nm) with Co-O-C-C-C-C-O-Co pathway, the system could be treated as magnetically isolated 1D chain. Variable-temperature magnetic susceptibility of **1** was carried out at 2 000 Oe and from 2.0 to 300 K on a polycrystalline sample. As shown in Fig.3, the $\chi_M T$ value at 300 K is 1.86 $cm^3 \cdot mol^{-1} \cdot K$, which is slightly lower than the expected value (1.88 $cm^3 \cdot mol^{-1} \cdot K$) of one magnetically isolated spin-only Co(Ⅱ) ion. As T is lowered, $\chi_M T$ continuously increases and reaches a local maximum of 5.02 $cm^3 \cdot mol^{-1} \cdot K$ at 14 K, and then dropping quickly to 1.69 $cm^3 \cdot mol^{-1} \cdot K$ at 2.0 K. This behaviour may indicate the occurrence of a weak ferromagnetic interaction.

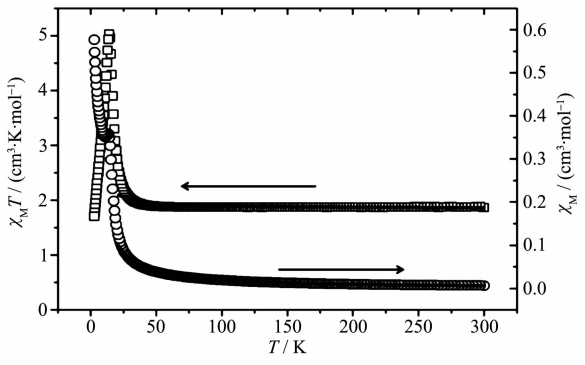


Fig.3　Plots of $\chi_M T$(□) and χ_M(○) versus T for **1**

The magnetic susceptibility in the range of 21~300 K obeys the Curie-Weiss law with a Curie constant C=3.01 $cm^3 \cdot mol^{-1} \cdot K$, which is close to the experimental value 3.39 $cm^3 \cdot mol^{-1} \cdot K$ for an octahedral Co(Ⅱ) ion, and a positive Weiss constant θ of 3.39 K. The Curie constant for spin-only Co(Ⅱ) ion is 1.875 $cm^3 \cdot mol^{-1} \cdot K$; the relatively bigger C value for **1** should arise from the significant spin-orbit coupling of Co(Ⅱ) ion. The positive θ value indicates dominating ferromagnetic interactions between the neighbouring Co(Ⅱ) ions via the Co-O-C-C-C-C-O-Co pathway. In order to understand quantitatively the magnitude of magnetic interaction, a 1D chain model has been utilized to simulate the experimental magnetic behavior. Then the interaction (J) can be expressed by the spin Hamiltonian $H=-J\sum S_i S_{i+1}$. In the classical-spin approximation, the following expression (Eq.**1**) of magnetic susceptibility was deduced by Fisher[18].

$$\chi_{chain}=\frac{Ng^2\beta^2 S(S+1)}{3kT}\left(\frac{1+\mu}{1-\mu}\right) \quad (1)$$

where μ is the Langevin function, $\mu=\coth[JS(S+1)/(kT)]-kT/[JS(S+1)]$, with S=3/2. The best simulation of the experimental data of **1** lead to J=0.72 cm^{-1}, g=1.99 with an agreement factor (defined as $R=\sum[(\chi_M)_{obs}-(\chi_M)_{calc}]^2/\sum(\chi_M)^2_{obs}$) of 8.5×10^{-3}. The solid lines in Fig.3 show

that the data in the 21~300 K rang are accommodated by Eq.**1**. The result indicates that there is a weak ferromagnetic interaction between Co(Ⅱ) ions in **1**.

Similar to structural analysis of compound **1**, there are 1D Cu(Ⅱ) chains with the Cu⋯Cu distance of 0.625 1 nm in compound **2**. Magnetic susceptibility of **2** was measured at 2 000 Oe and from 2.0 to 300 K on a polycrystalline sample. As shown in Fig.4, the $\chi_M T$ value at room temperature is 0.374 $cm^3 \cdot mol^{-1} \cdot K$, which is very close to the expected value for one uncoupled spin (C=0.374 $cm^3 \cdot mol^{-1} \cdot K$, S=1/2, g=2) of Cu(Ⅱ). As the temperature is lowered to 2 K, the $\chi_M T$ products decrease first slowly and then rapidly. This behavior suggests that antiferromagnetic interaction is operative in **2**. To simulate the experimental magnetic interactions in the system, we used the analytical expression for a one-dimensional Heisenberg chain of classical spins (S=1/2)[19]:

$$\chi_M=[Ng^2\beta^2/(kT)][(A+Bx+Cx^2)/(1+Dx+Ex^2+Fx^3)] \quad (2)$$

Where χ_M denotes the susceptibility per Cu(Ⅱ) compound, $x=|J|/(kT)$, A=0.25, B=0.149 95, C=0.300 94, D=1.986 2, E=0.688 54, and F=6.062 6.

The least-squares analysis of the magnetic susceptibility data led to J=−0.23 cm^{-1}, g=2.00, and R=1.1 ×10 $^{-3}$. The result indicates the typical feature of paramagnetic behavior in compound **2**.

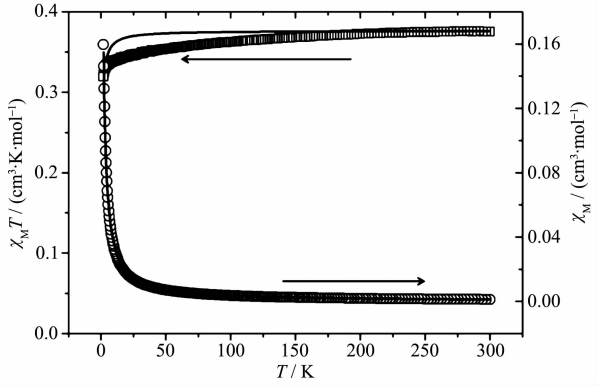


Fig.4 Plots of $\chi_M T$(□) and χ_M(○) versus T for **2**

3 Conclusions

In summary, two isomorphic compounds have been generated from mixed-ligands system of the 3-(1*H*-pyrazol-4-yl)-5-(pyridin-2-yl)-1,2,4-triazole and aromatic carboxylic acid ligands, which display the same 2D net. Aromatic carboxylic acids are introduced not only to balance the charge but also to coordinate with metal ions, with the aim of obtaining novel products. Accordingly, our present findings will further enrich the crystal engineering strategy and offer the possibility of controlling the formation of the desired network structures. Magnetic studies reveal weak ferromagnetic and paramagnetic behavior in **1** and **2**, respectively.

References:

[1] Cowan M G, Miller R G, Southon P D, et al. *Inorg. Chem.*, **2014**,**53**:12076-12083

[2] Goswami S, Adhikary A, Jena H S, et al. *Inorg. Chem.*, **2013**, **52**:12064-12069

[3] Zhang X, Sun M L, Huang Y Y, et al. *Inorg. Chem. Commun.*, **201**,**37**:155-157

[4] Feng X, Liu J, Chen J L, et al. *Inorg. Chem. Commun.*, **2014**, **50**:42-47

[5] Feng X, Chen J L, Li R F, et al. *Inorg. Chem. Commun.*, **2016**, **66**:41-46

[6] Huang Y M, Zhang B G, Duan J G, et al. *Cryst. Growth Des.*, **2014**,**14**:2866-2872

[7] Ward M D, Raithby P R. *Chem. Soc. Rev.*, **2013**,**42**:1619-1636

[8] Du M, Li C P, Liu C S, et al. *Coord. Chem. Rev.*, **2013**,**257**: 1282-1305

[9] TANG Hui(唐辉), GUO Yan-Hong(郭艳红), SHENG Jun-Feng(盛俊峰), et al. *Chinese J. Inorg. Chem.*(无机化学学报), **2017**,**33**(1):134-142

[10]Wang Y F, Li S H, Ma L F, et al. *Inorg. Chem. Commun.*, **2015**,**62**:42-46

[11]Guo X G, Yang W, Wu X, et al. *Dalton Trans.*, **2013**,**42**: 15106-15112

[12]Colombo V, Galli S, Choi H J, et al. *Chem. Sci.*, **2011**,**2**: 1311-1319

[13]Ganguly S, Mondal R. *Cryst. Growth Des.*, **2015**,**15**:2211-2222

[14]Ma L, Yu N Q, Chen S S, et al. *CrystEngComm*, **2013**,**15**: 1352-1364

[15]Chen K J, Lin R B, Liao P Q, et al. *Cryst. Growth Des.*, **2013**,**13**:2118-2123

[16]Sheldrick G M. *Acta Crystallogr. Sect. A*: *Found. Crystallogr.*, **2008**,**A64**:112-122

[17]Wang Y F, Li Z, Sun Y C, et al. *Inorg. Chem. Commun.*, **2014**,**44**:25-28

[18]Fisher M E. *Am. J. Phys.*, **1964**,**32**:343-346

[19]Ma L F, Wang Y Y, Wang L Y, et al. *Eur. J. Inorg. Chem.*, **2008**:693-703